2018 21st International Conference on Intelligent Transportation Systems (ITSC)
Maui, Hawaii, USA, November 4-7, 2018

Trajectory Planning for Autonomous Highway Driving Using the Adaptive Potential Field

Dongchan Kim, Hayoung Kim and Kunsoo Huh, *Member, IEEE*

***Abstract*— In this paper, we propose a novel autonomous highway driving framework using optimal trajectory generation with an adaptive potential field model. While the existing potential field models for trajectory generation are hard to consider dynamic aspects of obstacles, the proposed potential field model overcomes such limitation by changing the risk size of the potential field. To express the risk function of moving object, the constant time gap policy is utilized. By combining the adaptive potential field and optimal trajectory generation scheme, the proposed driving framework successfully makes autonomous vehicles perform a variety of highway driving functionalities such as lane keeping, lane changing, distance keeping and collision avoidance in critical situations.**

I. INTRODUCTION

Autonomous driving aims to recognize a surrounding environment and travel to the desired destination safely without the driver's intervention while following the road regulations. Autonomous driving will effectively reduce traffic violation and speeding because traffic law restricts a safe distance between cars. It will also prevent accidents caused by carelessness of drivers, which accounts for the majority of the casualties [1], [2].

A lot of research has been conducted for decades to develop autonomous driving technology and great accomplishment is being made. It is also identified as the ultimate goal of advanced driver assistance systems (ADAS) [3]. The factors that compose autonomous driving technology are diverse, and the trajectory generation part takes an important role.

Researchers around the world have sought to develop an efficient and safe trajectory planning method for autonomous driving, and numerous studies have been conducted accordingly. Recently, a lot of research is dealing with dynamic environment. In order to ensure safety, trajectory planning with respect to time is important considering the dynamic environment. Most of the research on this topic deals with techniques for generating optimized trajectories and can be conceptually divided into two approaches [4]: direct optimization method and indirect optimization method. The direct optimization methods mainly deal with Model Predictive Control (MPC) [5]–[7]. MPC-based trajectory planning solves an optimization problem that sets a cost function and satisfies a desired set of constraints during finite-time. This approach has drawbacks of computing cost and proof of convergence.

Dongchan Kim, Hayoung Kim and Kunsoo Huh are with the Department of Automotive Engineering, Hanyang University, Seoul, 04763, Republic of Korea. jookker,hayoung.kim,khuh2@hanyang.ac.kr

In the indirect optimization method, there are many studies using polynomials among the sampling-based methods to generate trajectories [8]–[13]. These methods set various constraints associated with vehicle kinematics and dynamics to obtain a feasible trajectory set. Then, a suboptimal solution is found in the discrete solution space. This approach has an advantage that the computing cost is relatively small, and the convergence is guaranteed.

This study aims at performing safe path generation in highway scenario. Here, we propose a method of combining the adaptive potential field model with the existing method. The cost function of the optimization problem is expressed as a sum of several terms and is non-convex. In order to approach this problem easily, an indirect optimization method is used. Using the potential field model, the surrounding environment can be effectively expressed, and the most important surrounding vehicle model can be designed in various ways [14]–[16]. In this study, we propose a method to adaptively express the potential field model of the surrounding vehicle by utilizing the conventional constant-time-gap policy. In the existing method [8], two types of trajectory generation are performed according to the purpose, so a suitable mode selection mechanism is required. In this study, the target highway scenarios are considered with one trajectory generation method.

The contents of the paper are composed as follows. Section 2 presents the overall framework of the proposed algorithm. The description of the adaptive potential field model and the trajectory planning algorithm using the model are explained. Section 3 evaluates the proposed trajectory planner through simulation. Finally, Section 4 provides the conclusion.

II. ALGORITHM FRAMEWORK

In order to generate the trajectory in a highway road, it is necessary to consider various surrounding conditions such as vehicles, road information, speed regulation, etc. Based on understanding the situations, autonomous vehicles must maintain speed, change lanes, and runs safely without colliding with surrounding vehicles. Therefore, the final trajectory should be determined considering safety, comfort and limits of the vehicle dynamics.

The framework of the proposed algorithm is shown in Fig. 1. First, it receives information about the surrounding environment such as relative position and relative velocity of the surrounding vehicles. It also receives own vehicle information such as position and velocity, and map information of the road to be driven. It is assumed that the information used is ideally obtained in real-time. Using this information, the

978-1-7281-0322-8/18/$31.00 ©2018 IEEE

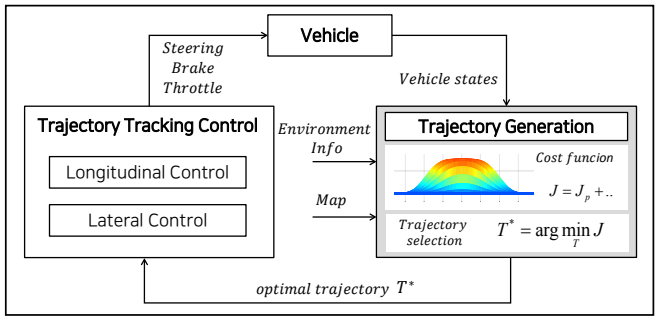

Fig. 1. Algorithm framework for trajectory planning and control.

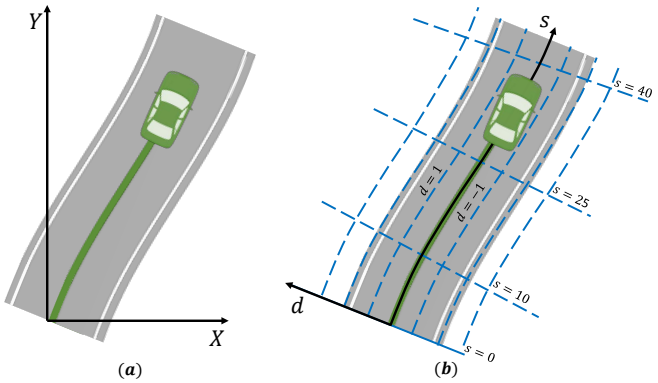

Fig. 2. Frenet coordinates of road geometry. (a) Cartesian coordinates (b) Frenet coordinates.

optimal trajectory is selected by the carefully designed cost function through the sampling-based trajectory generation process. At this time, the process is described in the so-called the Frenet coordinates as shown in Fig. 2. Finally, in the trajectory tracking control part, longitudinal and lateral control are performed. This paper focuses mainly on the trajectory planner part.

A. Potential Field Design

The potential field is designed considering three factors [17]: the surrounding vehicles, the road boundaries and the centerline of the lane. The surrounding vehicle model restricts the approach of the ego vehicle, and the road boundary model prevents the vehicle from selecting the trajectory near the road boundary. Finally, the lane centering model leads the ego vehicle to the centerline of the lane. The path of the surrounding vehicle is predicted using the constant velocity model on the Frenet coordinates. Because the potential field related to the surrounding vehicle is different from [17], this part is described in detail.

As described in [17] for the surrounding vehicle model, s-direction risk magnitude can be changed to the desired shape by making the value of σ_{vehs} variable. As shown in Fig.3, the distance $2\sigma_{vehs}$ from the center of the surrounding vehicle can be assumed to represent the whole model. Therefore, this $2\sigma_{vehs}$ value can be used as a distance that the ego vehicle wants to keep between the surrounding vehicle. The conventional constant-time-gap policy [18] is used to get a reference distance with the surrounding vehicle as follows:

$$s_{ref}(t) = D_0 + \tau \dot{s}(t) \tag{1}$$

where D_0 and τ are design parameters. Then, σ_{vehs} can be derived as

$$\sigma_{vehs} = \frac{s_{ref}(t)}{2} \tag{2}$$

Substituting (1) and (2) into (3) produces an adaptive potential field of the surrounding vehicle for the safe distance.

$$P_{veh_i}(k\,|t) = A_{veh} \exp\left(-\left(\frac{(s(k|t) - s_{veh_i}(k|t))^2}{2{\sigma_{vehs_i}}^2} + \frac{(d(k|t) - d_{veh_i}(k|t))^2}{2{\sigma_{vehd_i}}^2}\right)^c\right)$$
$$for \quad k = t+1, \ldots, t+N_{path} \tag{3}$$

where P_{vehi} : potential field of ith surrounding vehicle
A_{veh}: maximum value of the vehicle potential field
N_{path}: number of path horizon
s, d: ego vehicle positions in the Frenet coordinates
s_{veh_i}, d_{veh_i}: i^{th} vehicle positions
$\sigma_{vehs_i}, \sigma_{vehd_i}, c$: variables that determine the shape of the potential field

Fig.4 shows an example image of a total sum of all the potential field models.

B. Trajectory Generation

1) Restrictions: Vehicle motion is not considered when sampling-based polynomial trajectory generation is carried out. Therefore, it is necessary to exclude candidates that do not satisfy various constraints about vehicle kinematics and dynamics. It is also important to keep the rules of the road. In this part, after the longitudinal and lateral trajectories are created separately in the Frenet coordinates, several restrictions are checked.

Prior to combining the longitudinal and lateral trajectories, only the candidates which satisfy the velocity constraint are included. For the comfort and safety of the driver, s-axis velocity in the road direction is limited. First, the maximum lateral acceleration $\ddot{d}_{\max}$ which considers the driving comfort is set. Then, with the information about the road curvature κ, the velocity limit $\dot{s}_{limit}$ is calculated by

$$\dot{s}_{limit} = \sqrt{\frac{\ddot{d}_{\max}}{\kappa}} \tag{4}$$

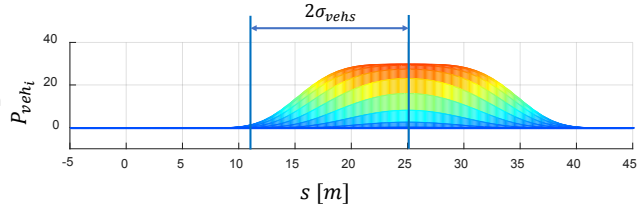

Fig. 3. Side view of the surrounding vehicle potential field.

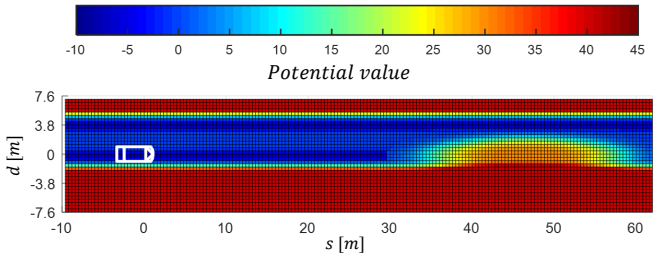

Fig. 4. Example of a combined potential field

Since the curvature is small on the straight line, the value from (4) could become very large. Therefore, the recommended velocity of the road $\dot{s}_{road}$ is set. Then, the reference longitudinal velocity $\dot{s}_{set}$ is simply determined by

$$\dot{s}_{set} = min(\dot{s}_{limit}, \dot{s}_{road}) \tag{5}$$

After combining the longitudinal and lateral trajectory sets, curvature confirmation is performed for vehicle kinematic constraint check. Curvature of the trajectory is limited by the steering geometry of the vehicle, and its constraint is defined as

$$\kappa_{cand} \in [\kappa_{min}, \kappa_{max}] \tag{6}$$

Next, limitations are given to longitudinal and lateral acceleration values, taking into account the physical limitations of the vehicle dynamics. This limit is from a circle of forces [19], and accelerations in s and d-axis are used as follows:

$$\ddot{s}(t)^2 + \ddot{d}(t)^2 \leq a^2{}_{max} \tag{7}$$

Finally, collision check with other vehicles is performed. For this process, the vehicle is represented by two circles in the manner of [20], then a separate collision check is performed for each trajectory candidate. Unlike [11] all the restrictions are checked on the Frenet coordinates, not on Cartesian coordinates.

2) Trajectory Planning by 4^{th} and 5^{th} Order Polynomials: Trajectory planning in the Frenet coordinates has an advantage of planning longitudinal and lateral trajectories separately. The longitudinal ones are placed on the s-axis which is the direction of the road, and the lateral ones on the d-axis which are perpendicular to the s-axis. After longitudinal and lateral trajectories are generated and the optimal one is selected, the final trajectory is transformed back to the Cartesian coordinates for control purpose.

We use a similar approach as [8] and generate trajectory candidates using polynomials in time domain. A quartic polynomial is used for the longitudinal direction and a quintic polynomial is used for the lateral direction as follows:

$$\begin{aligned} s(t) &= \alpha_0 + \alpha_1 t + \alpha_2 t^2 + \alpha_3 t^3 + \alpha_4 t^4 \\ d(t) &= \beta_0 + \beta_1 t + \beta_2 t^2 + \beta_3 t^3 + \beta_4 t^4 + \beta_5 t^5 \end{aligned} \tag{8}$$

In order to solve the polynomial function in s-direction, three initial states and two final states $[s_i, \dot{s}_i, \ddot{s}_i, \dot{s}_f, \ddot{s}_f]$ are used without position information at final states. To make various trajectory candidates, final constraints are varied by different $\Delta\dot{s}_m$ and time interval T_n according to

$$[\dot{s}_f, \ddot{s}_f, T]_{mn} = [[\dot{s}_{ref} + \Delta\dot{s}_m], 0, T_n] \tag{9}$$

In the case of $\dot{s}_{ref}$ used in (9), if the ego vehicle is behind the leading vehicle in the same lane, it is determined as follows:

$$\begin{aligned} &if\ \max\left(P_{veh_i}\left(k\,|t\right)\right) > P_{veh,thres},\ \ \dot{s}_{ref} = \dot{s}_{veh_i}, \\ &otherwise, \dot{s}_{ref} = \dot{s}_{set} \end{aligned} \tag{10}$$

where $\dot{s}_{veh_i}$: longitudinal velocity of i^{th} surrounding vehicle
$P_{veh,thres}$: potential value threshold of the vehicle

The above relation is to diversify the candidates of $\dot{s}_f$ in (9) based on the surrounding vehicle's velocity. This condition is applied when the ego vehicle approaches to the leading vehicle of the same lane and the potential risk becomes larger than a certain value. As a result, even with the velocity planning method (quartic polynomial), it is possible to generate smooth distance keeping candidates.

In the case of d-direction trajectories, three initial states and three final states $[d_i, \dot{d}_i, \ddot{d}_i, d_f, \dot{d}_f, \ddot{d}_f]$ are used. To make various trajectory candidates, final constraints are varied by different d_m and time interval T_n according to

$$[d_f, \dot{d}_f, \ddot{d}_f, T]_{mn} = [d_m, 0, 0, T_n] \tag{11}$$

Here, we set $\dot{d}_f = \ddot{d}_f = 0$ so that the last part of the trajectory becomes the road direction.

C. Optimal Trajectory Selection

The longitudinal and lateral trajectory sets are combined, and the optimal trajectory is selected among the candidates satisfying the restrictions. In order to select the optimal one, a cost function is defined, and it consists of four terms.

$$J_{tot} = w_s J_s + w_d J_d + w_c J_c + w_p J_p \tag{12}$$

The first cost term is for the optimization of the longitudinal movement and it considers the longitudinal jerk, the deviation from the reference velocity and the time interval:

$$J_s = c_{j,s} \int_{t_i}^{t_f} (\dddot{s}(t))^2 dt + c_{v,s}(\dot{s}_{set} - \dot{s}_f)^2 + c_{T,s} T \tag{13}$$

where $c_{j,s}$, $c_{v,s}$, $c_{T,s}$ are weights for each index.

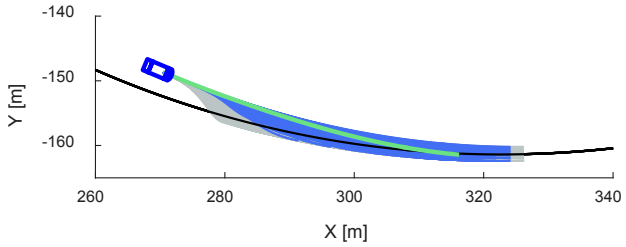

Fig. 5. Example of a set of planned trajectories toward the center line: invalid(gray), valid(blue), optimal(green). The set is superposition of the longitudinal and lateral trajectories.

The second cost term is for the optimization of the lateral movement and it considers the lateral jerk and the time interval:

$$J_d = c_{j,d} \int_{t_i}^{t_f} (\dddot{d}(t))^2 dt + c_{T,d} T \tag{14}$$

where $c_{j,d}$, $c_{T,d}$ are weights for each index.

The third cost term is for the consistency of the consecutive re-plans. The inconsistency between the re-plans could result in oscillations of the trajectories and thus, the terminal lateral deviation is considered:

$$J_c = (d_f - d_{f,opt})^2 \tag{15}$$

where $d_{f,opt}$ is from the previously selected optimal trajectory.

The last cost term consists of the potential field models explained in Section 2-A:

$$J_p = \sum_{k=t+1}^{t+N_{path}} \left\{ \sum_i P_{veh_i}(k\,|t) + \sum_j P_{rb_j}(k\,|t) + \sum_l P_{ctr_l}(k\,|t) \right\} \tag{16}$$

where P_{rb_j}: potential field of j^{th} road boundary [17]
P_{ctr_l}: potential field of l^{th} lane centerline [17]

Fig. 5 shows the resulting trajectory set toward the center line. The gray lines are invalid trajectories by the restrictions and the blue lines are valid trajectories. And the green line is the selected trajectory through the cost function.

III. Simulation and Results

The proposed algorithm is verified in simulations with *MATLAB/Simulink* and *CarSim*. A total of two different scenarios are constructed by arranging the vehicles with various velocities and motions on the same road model. The first scenario consists of normal driving situations and verifies the performance of lane keeping, lane changing and distance keeping. The second scenario consists of a situation in which the surrounding vehicles are running in a threatening manner especially an abrupt cut-in motion. In addition, this scenario verifies the performance of collision avoidance in two situations where either an evasive trajectory or a braking trajectory is required. The combined steering and braking/acceleration are used in control.

A. Normal Highway Driving

1) Lane Keeping: Fig. 6-10 show the screen captures of each scenario, and all the figures are presented in birds eye view. The blue line stemming from the ego vehicle represents the selected optimal trajectory. And the lines stemming from the surrounding vehicles represent the predicted motions. In Fig. 6, there is no surrounding vehicle nearby, so the ego vehicle keeps the lane with the desired velocity $\dot{s}_{set}$.

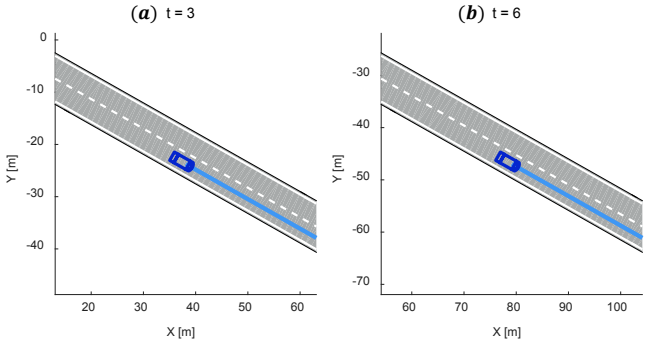

Fig. 6. Lane keeping maneuver.

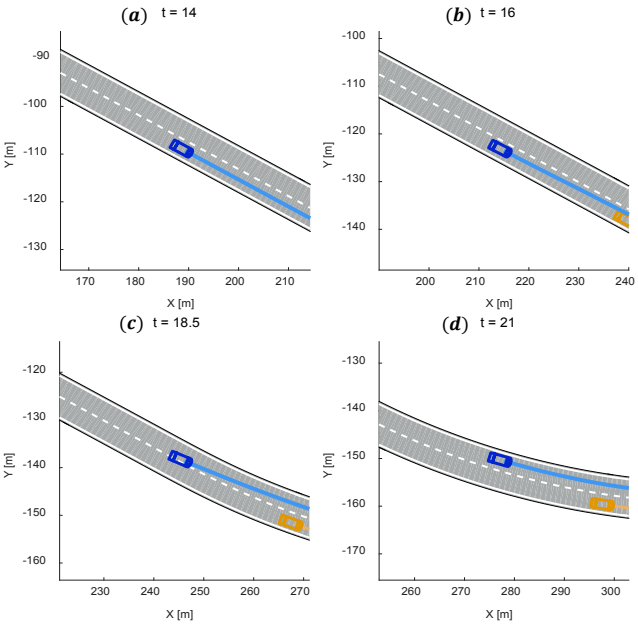

Fig. 7. Lane keeping and lane changing maneuvers: The ego vehicle (a) keeps the lane; (b) decreases the velocity a little behind the slowly moving leading vehicle and chooses a lane change trajectory; (c) performs lane change; (d) increases the velocity and keeps the lane.

2) Lane Changing: Fig. 7 shows performing lane change. At the beginning, lane keeping is carried out and the ego vehicle meets a slowly moving leading vehicle as shown in Fig. 7(b). The ego vehicle changes the lane while slightly slowing down the velocity (Fig. 7(c)). Then, in the changed left lane, the ego vehicle performs lane keeping again and speeds up to $\dot{s}_{set}$ (Fig. 7(d)). Here, with the cost weights $w_s \approx w_d$, the ego vehicle prefers to perform distance keeping behind the leading vehicle. And with $w_s \gg w_d$, the ego vehicle prefers to pass slower vehicles and this is the case in the simulations.

3) Distance Keeping and Lane Changing: Fig. 8 shows performing distance keeping and lane changing at the end of the scenario. Fig. 8 (a) and (b) show situations where the ego vehicle meets slower leading vehicles. Here, the ego vehicle slows down than the reference velocity $\dot{s}_{set}$ and follows the leading vehicle (red) with distance keeping. Then, as shown in Fig. 8(c), when the leading vehicle (red)

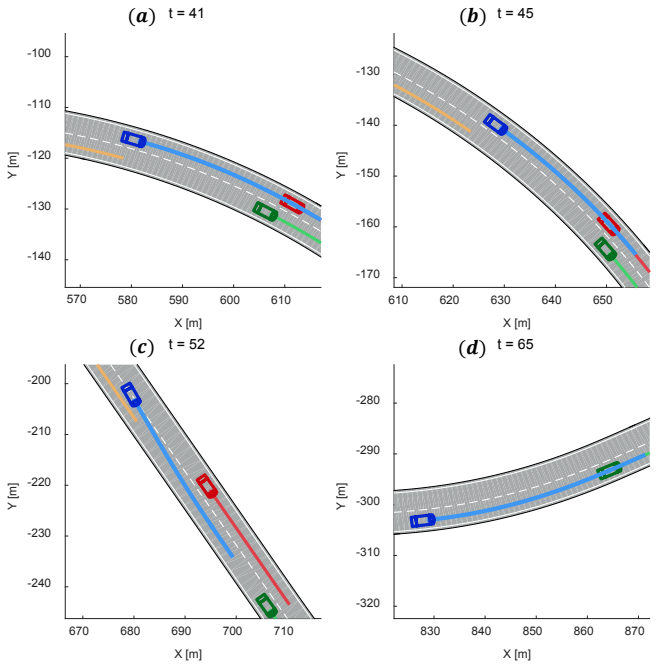

Fig. 8. Distance keeping and lane changing maneuvers: The ego vehicle (a) and (b) first keeps the distance from the slowly moving front vehicle(red); (c) performs a lane change after the leading vehicle(red) decreases velocity; (d) increases the velocity and keeps the distance from the preceding vehicle(green).

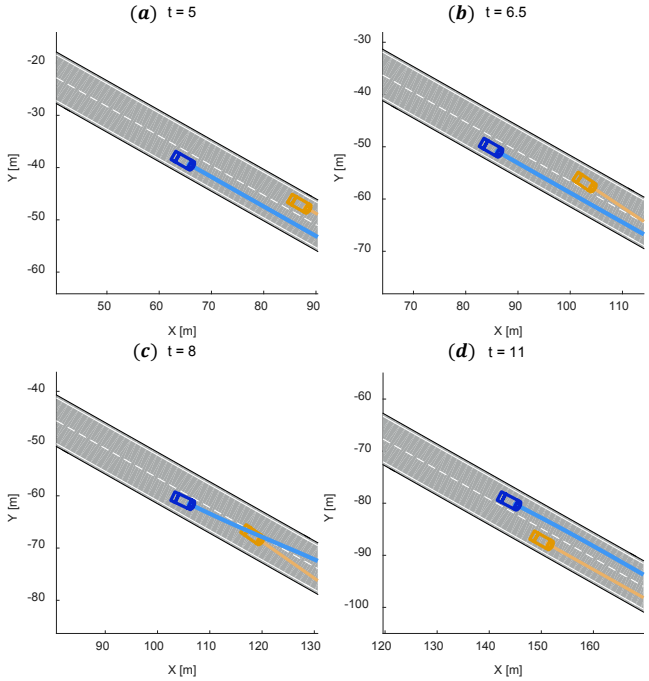

Fig. 9. Collision avoidance through evasive trajectory: (a) The ego vehicle keeps the lane; (b) The surrounding vehicle attempts cut-in into the ego lane; (c) and (d) The ego vehicle avoids collision by steering.

slows down the speed and the right lane is open, the ego vehicle tries to change lane. The vehicle accelerates toward $\dot{s}_{set}$ and meets another leading vehicle (green) with only a little velocity difference. At this time, the vehicle performs distance keeping.

B. Severe Highway Driving

1) Collision Avoidance Through Evasive Trajectory: Fig. 9 shows the situation when the surrounding vehicle attempts cut-in into the ego lane and the other lane is empty. As can be seen in Fig. 9(c) and (d), the ego vehicle avoids collision through the evasive maneuver to the left lane. Although combined steering and braking/acceleration are used, steering plays a big role in this situation.

2) Collision Avoidance Through Braking Trajectory: Fig. 10 shows the situation when one (red) of the surrounding vehicles attempts cut-in into the ego lane and no lane is empty. As can be seen in Fig. 10(c), the ego vehicle avoids collision in the ego lane because lane change could result in collision with another surrounding vehicle (green). At this time, braking plays a big role. After avoiding the danger, the ego vehicle keeps a proper distance from the leading vehicle (red) as shown in Fig. 10(d).

IV. Conclusion

We present a novel autonomous highway driving framework, in which an optimal trajectory generation scheme is integrated with the adaptive potential field model. The constant-time-gap policy is utilized to express the potential field model of surrounding vehicles. All the target scenarios are verified in simulations with respect to two scenarios, normal driving and severe driving. The purpose is to evaluate the performance of lane keeping, lane changing, distance keeping and collision avoidance in both scenarios, and the results show that the proposed algorithm works well in all the situations. Future work will focus on verification of more diverse scenarios and implementation of the trajectory planner in real experiment.

Acknowledgment

This research was supported by Korea Evaluation Institute of Industrial Technology(KEIT) grant funded by the Korea government(MOTIE) (No. 10052375, Test Scenario Study for Supporting Autonomous Driving Technology Development).

This work was also supported by the Industrial Strategic Technology Development Program(10079730, Development and Evaluation of Automated Driving Systems for Motorway and City Road) funded By the Ministry of Trade, Industry Energy(MOTIE, Korea)

References

[1] V. Beanland, M. Fitzharris, K. L. Young, and M. G. Lenné, "Driver inattention and driver distraction in serious casualty crashes: Data from the australian national crash in-depth study," *Accident Analysis & Prevention*, vol. 54, pp. 99–107, 2013.

[2] N. H. T. S. Administration *et al.*, "2015 motor vehicle crashes: overview," *Traffic safety facts research note*, vol. 2016, pp. 1–9, 2016.

[3] K. Bengler, K. Dietmayer, B. Farber, M. Maurer, C. Stiller, and H. Winner, "Three decades of driver assistance systems: Review and future perspectives," *IEEE Intelligent Transportation Systems Magazine*, vol. 6, no. 4, pp. 6–22, 2014.

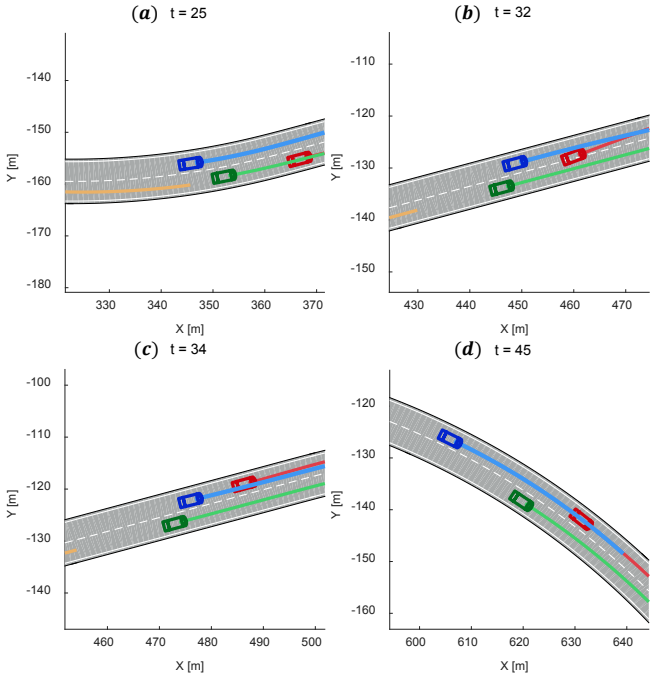

Fig. 10. Collision avoidance through braking trajectory: (a) The ego vehicle keeps the lane; (b) One (red) of the leading vehicles attempts cut-in into the ego lane; The ego vehicle (c) avoids collision by braking; (d) keeps the distance from the leading vehicle.

[4] C. Rathgeber, F. Winkler, X. Kang, and S. Müller, "Optimal trajectories for highly automated driving," *World Academy of Science, Engineering and Technology, International Journal of Mechanical, Aerospace, Industrial, Mechatronic and Manufacturing Engineering*, vol. 9, no. 6, pp. 969–975, 2015.

[5] A. Gray, Y. Gao, T. Lin, J. K. Hedrick, H. E. Tseng, and F. Borrelli, "Predictive control for agile semi-autonomous ground vehicles using motion primitives," in *American Control Conference (ACC), 2012*. IEEE, 2012, pp. 4239–4244.

[6] M. Jalalmaab, B. Fidan, S. Jeon, and P. Falcone, "Model predictive path planning with time-varying safety constraints for highway autonomous driving," in *Advanced Robotics (ICAR), 2015 International Conference on*. IEEE, 2015, pp. 213–217.

[7] C. Liu, S. Lee, S. Varnhagen, and H. E. Tseng, "Path planning for autonomous vehicles using model predictive control," in *Intelligent Vehicles Symposium (IV), 2017 IEEE*. IEEE, 2017, pp. 174–179.

[8] M. Werling, J. Ziegler, S. Kammel, and S. Thrun, "Optimal trajectory generation for dynamic street scenarios in a frenet frame," in *Robotics and Automation (ICRA), 2010 IEEE International Conference on*. IEEE, 2010, pp. 987–993.

[9] P. Resende and F. Nashashibi, "Real-time dynamic trajectory planning for highly automated driving in highways," in *Intelligent Transportation Systems (ITSC), 2010 13th International IEEE Conference on*. IEEE, 2010, pp. 653–658.

[10] W. Xu, J. Wei, J. M. Dolan, H. Zhao, and H. Zha, "A real-time motion planner with trajectory optimization for autonomous vehicles," in *Robotics and Automation (ICRA), 2012 IEEE International Conference on*. IEEE, 2012, pp. 2061–2067.

[11] M. Werling, S. Kammel, J. Ziegler, and L. Gröll, "Optimal trajectories for time-critical street scenarios using discretized terminal manifolds," *The International Journal of Robotics Research*, vol. 31, no. 3, pp. 346–359, 2012.

[12] A. Goswami, "Trajectory generation for lane-change maneuver of autonomous vehicles," Ph.D. dissertation, Purdue University, 2015.

[13] X. Li, Z. Sun, D. Cao, Z. He, and Q. Zhu, "Real-time trajectory planning for autonomous urban driving: framework, algorithms, and verifications," *IEEE/ASME Transactions on Mechatronics*, vol. 21, no. 2, pp. 740–753, 2016.

[14] M. T. Wolf and J. W. Burdick, "Artificial potential functions for highway driving with collision avoidance," in *Robotics and Automation, 2008. ICRA 2008. IEEE International Conference on*. IEEE, 2008, pp. 3731–3736.

[15] Q. Tu, H. Chen, and J. Li, "A potential field based lateral planning method for autonomous vehicles," *SAE International Journal of Passenger Cars-Electronic and Electrical Systems*, vol. 10, no. 2016-01-1874, pp. 24–34, 2016.

[16] Y. Rasekhipour, A. Khajepour, S.-K. Chen, and B. Litkouhi, "A potential field-based model predictive path-planning controller for autonomous road vehicles," *IEEE Transactions on Intelligent Transportation Systems*, vol. 18, no. 5, pp. 1255–1267, 2017.

[17] D. Kim, H. Kim, and K. Huh, "Local trajectory planning and control for autonomous vehicles using the adaptive potential field," in *Control Technology and Applications (CCTA), 2017 IEEE Conference on*. IEEE, 2017, pp. 987–993.

[18] R. Rajamani, *Vehicle dynamics and control*. Springer Science & Business Media, 2011.

[19] H. Pacejka, *Tire and vehicle dynamics*. Elsevier, 2005.

[20] W. Lim, S. Lee, M. Sunwoo, and K. Jo, "Hierarchical trajectory planning of an autonomous car based on the integration of a sampling and an optimization method," *IEEE Transactions on Intelligent Transportation Systems*, vol. 19, no. 2, pp. 613–626, 2018.